IMA Journal of Numerical Analysis (1999) **19**, 1–??

An Unconditionally Stable Splitting Scheme for a Class of Nonlinear Parabolic Equations

KENNETH HVISTENDAHL KARLSEN†
Department of Mathematics, University of Bergen
Johs. Brunsgt. 12, N–5008 Bergen, Norway
AND
KNUT–ANDREAS LIE†
Department of Informatics, University of Oslo
P.O. Box 1080 Blindern, N–0316 Oslo, Norway

[Received xx April 199x and in revised form xx August 199x]

We propose and analyse a numerical scheme for a class of advection dominated advection–diffusion–reaction equations. The scheme is essentially based on operator splitting combined with a *front tracking* method for conservation laws, which tracks an evolving piecewise constant solution with discontinuity paths defined by a varying velocity field. The splitting separates out the advection, which is modelled by a nonlinear conservation law, and the diffusion/reaction. Since the front tracking scheme (unlike conventional methods) has no associated time step, our numerical scheme can be made unconditionally stable by choosing appropriate methods for the diffusion and reaction steps. Nevertheless, it is observed that when the time step is notably larger than the diffusion scale, the scheme can become too diffusive. This can be inferred with the fact that the entropy condition forces the hyperbolic solver to throw away information (entropy loss) regarding the structure of steep fronts. We will demonstrate that the disregarded information can be identified as a residual flux term. Moreover, if this residual flux is taken into account via, for example, a separate *correction* step, steep fronts can be given the correct amount of self sharpening. Four numerical examples are presented. The first three examples discuss the quality of the approximate solutions in terms of accuracy and efficiency. The last example is drawn from glacier modelling.

1. Introduction

Mathematical models that involve a combination of advective, diffusive, and reactive processes are among the most widespread in all of sciences, engineering, and other fields where mathematical modelling is important. Applications range from models of turbulence (Burgers (1974)), via traffic flow (Lighthill & Whitham (1955)) and modelling of share options on the financial market (Black & Scholes (1973)), to multi-phase flow in porous media (Trangenstein (1995)). Other applications include, to mention a few, polymer chemistry (Chella & Ottino (1983)),

† Research for this article was carried out while Karlsen was visiting the Institute for Mathematics and its Applications (IMA), University of Minnesota. Karlsen thanks IMA for financial support and great hospitality. Karlsen has also been supported by VISTA, a research cooperation between the Norwegian Academy of Science and Letters and Den norske stats oljeselskap a.s. (Statoil). Lie has been supported by the Research Council of Norway under grant 100555/410.

© Oxford University Press 1999

combustion modelling (Mohanty *et al* (1982)), modelling of semi-conductor devices (Mock (1983)), and contaminant transport in groundwater and surface water (Bear & Verruijt (1987)).

We consider a class of nonlinear advection–diffusion–reaction equations of the form

$$\frac{\partial u}{\partial t} + \frac{\partial F(x,t,u)}{\partial x} = \varepsilon \frac{\partial^2 u}{\partial x^2} + G(x,t,u), \qquad (x,t) \in Q_T \equiv \mathbb{R} \times \langle 0, T], \qquad (1)$$

with initial data u_0 imposed at $t = 0$. Here the flux function F and the reaction/source/sink term G are bounded, smooth functions of all their arguments and the initial data u_0 is of bounded total variation.

When (1) is advection dominated, conventional numerical methods exhibit some combination of difficulties, ranging from non-physical oscillations (central difference/Galerkin schemes) to excessive numerical diffusion (upwind schemes) at steep fronts. In the last two decades we have seen a tremendous activity on developing sophisticated numerical schemes that are designed to accurately capture *discontinuous solutions* of hyperbolic conservation laws; see for instance, Godlewski & Raviart (1996), Holden & Risebro (1998), and LeVeque (1992). It may therefore seem reasonable to employ some of these methods as "building blocks" in numerical schemes for advection–diffusion–reaction problems, at least for those that are of advection dominated nature.

A natural strategy is to split the equation into a hyperbolic conservation law modelling advection and a parabolic equation modelling diffusion and lower order terms (or also separate these two effects), and then try to reproduce the solution using these simpler equations as building blocks. Variations on this operator splitting approach have indeed been taken by several authors, we mention Demkowitz & Oden (1986), Douglas & Russell (1982), Espedal & Ewing (1987), Dahle (1988), and Arbogast & Wheeler (1995). A more general approach is the Eulerian–Lagrangian localized adjoint methods of Celia *et al* (1990), and Wang *et al*. See Dawson *et al* (1994), Ewing (1991), Ewing & Russell (1982), Herrera *et al* (1993), Russell (1983), Russell & Trujillo (1990), Wang *et al* (1995), and the references therein, for more details on this type of methods, which are all based on some kind of time stepping along the characteristics to realize the hyperbolic part of (1). Dawson (1991), Dawson (1995), and Wheeler *et al* (1988) employ Godunov (or upwind) methods to realize the hyperbolic part of (1), giving an approach closer to the one we advocate here. We also mention the recent work of Cockburn & Shu (1998) on the (unsplit) local discontinuous Galerkin method, which is an extension of the Runge-Kutta discontinuous Galerkin method for hyperbolic conservation laws.

The purpose of our paper is to continue and improve the work initiated recently on the corrected operator splitting (COS) approach; see Karlsen & Risebro (1997), Karlsen *et al*, and Karlsen *et al* (1998). This approach is based on a front tracking method for conservation laws and a *dynamical splitting* of the partial differential equation (1). Here we extend the method to include velocity fields and source terms. An ultimate goal is to accurately and effectively solve the partial differential equations describing multi-phase flow in porous media, including the strongly heterogeneous case where the coefficients in (1) vary discontinuously with the space

variable. Although we will use a simple linear diffusion term εu_{xx}, a nonlinear and possibly strongly degenerate diffusion term $\varepsilon(d(x,t,u)u_x)_x$ could have been considered. But in the degenerate case, weak solutions must be sought and they are, in general, not uniquely determined by their data. Consequently, an entropy condition must be imposed to pick out the physical weak solution. The use of entropy conditions (integral inequalities) are outside the scope of this paper, and we refer instead to Evje & Karlsen for details in the case $F \equiv f(u)$ and $G \equiv 0$.

We restrict ourselves to a (physically reasonable) class of equations in which the flux function F has the form $F(x,t,u) = V(x,t)f(u)$. This will enable us to write the parabolic equation (1) in the non-conservative form

$$u_t + V(x,t)f(u)_x = \varepsilon u_{xx} + Q(x,t,u), \tag{2}$$

where $Q(x,t,u) = G(x,t,u) - f(u)V_x(x,t)$. This equation will be our starting point for constructing approximate solutions. The non-conservative form is natural when seeking to define an operator splitting because the term $f(u)V_x$ represents accumulation and should therefore be grouped with the source G. Furthermore, the front tracking method we will use for the advective part seeks solutions that are constant within polygons defined by discontinuity paths and is accordingly defined for a non-conservative equation *without* accumulation terms, see §2.

Let $\mathcal{S}(t)$, $\mathcal{H}(t)$, and $\mathcal{R}(t)$ denote the solution operators associated with the hyperbolic equation $v_t + V(x,t)f(v)_x = 0$, the parabolic equation $w_t = \varepsilon w_{xx}$, and the ordinary differential equation $z_t = Q(x,t,z)$, respectively. Then the basic splitting takes the form

$$u(x, n\Delta t) \approx \left[\mathcal{R}(\Delta t) \circ \mathcal{H}(\Delta t) \circ \mathcal{S}(\Delta t)\right]^n u_0. \tag{3}$$

In the numerical method we will replace $\mathcal{S}(t)$ with a front tracking method, $\mathcal{H}(t)$ with an explicit difference scheme, and $\mathcal{R}(t)$ with the forward–Euler method. Note, that the main emphasis in this paper will be on front tracking and the corrected operator splitting. Consequently, our choice of numerical schemes for $\mathcal{H}(t)$ and $\mathcal{R}(t)$ will be very simple to allow us to focus on the main ideas of our solution strategy as well as keeping the details in the convergence analysis at a minimum.

The front tracking method we will use was first introduced by Dafermos (1972), then suggested as a numerical method by Holden *et al* (1988), and later extended to systems by Risebro (1993). Our method deviates slightly from the original (Holden *et al* (1988)) in that we track shock curves in a piecewise linear velocity field, yielding curves that vary piecewise exponentially in time as opposed to piecewise linearly. Applying front tracking for the advective step has some striking advantages. First, the method is unconditionally stable in the sense that there is no CFL condition restricting the time step and it is very efficient for scalar equations. Hence, arbitrary large time steps can be used in the splitting scheme. Second, as we shall see later, the method easily allows for a dynamical splitting of the equation (2), which contrasts the fixed splitting (3) that is usually employed; see Dawson (1991), Dawson (1995), or Karlsen & Risebro (1997). Although unconditionally stable, the method contains splitting errors. This means that a reasonable choice of Δt is highly dictated by the degree of interplay between advective, diffusive, and reactive forces. Here we will focus on the interaction between advection and diffusion. A thorough discussion of

the influence from reactive terms is left to a separate report. Instead, we refer to Crasta & Piccoli (1997), Holden & Risebro (1997), (Langseth *et al* 1996), Wang & Ewing (1995), and Wang *et al* (1995). These papers discuss the process of splitting off lower order terms in hyperbolic and parabolic conservation laws.

Let us for the moment assume that $Q \equiv 0$ so that (2) is of advection–diffusion type. When Δt is larger than the diffusion scale ε, we have observed that the splitting (3) is too diffusive near steep fronts (Karlsen *et al*, Karlsen & Risebro (1997)). The reason for this behaviour is that a convexification of the flux function is introduced locally (due to an entropy condition) in the advection step $\mathcal{S}(\Delta t)$. The structure of self-sharpening parabolic fronts is controlled by the local residual, i.e., the difference between the flux function and its convexification, which is thrown away in the (hyperbolic) solution process. Fortunately, we can compensate for this "loss of information" (unphysical entropy loss).

Assume that the solution of (2) is simply a moving steep front. Applying $\mathcal{S}(\Delta t)$ gives a discontinuity, with left and right limits u_l and u_r, respectively. Then we can identify the residual term as $f_{\text{res}} = f - f_c$, where f_c denotes the correct envelope (dictated by the entropy condition) of f on the interval bounded by u_l and u_r. There are several ways to take the residual flux term f_{res} into account. We can, for instance, perform a separate correction step after the diffusion step. Correction is then realized by solving the "residual" conservation law $v_t + V(x,t) f_{\text{res}}(v)_x = 0$ over a time interval $\langle 0, \tau]$, where $\tau > 0$ is some parameter that has to be chosen. Another approach is to include the residual term in the equation modelling diffusion, that is, instead of solving (only) the heat equation $w_t = \varepsilon w_{xx}$, we solve $w_t + V(x,t) f_{\text{res}}(w)_x = \varepsilon w_{xx}$. This equation contains the necessary information needed to produce the correct structure of the steep front, but contains a less severe nonlinearity than (2). We will here mainly discuss the first approach. But to demonstrate the potential of the second approach, numerical examples are presented where we compare these two slightly different corrected operator splitting schemes.

A simpler form of the techniques developed here has been implemented in a two-dimensional prototype two-phase reservoir simulator (Karlsen *et al* (1998)). The idea is to treat multi-dimensional equations by means of dimensional splitting. To be more precise, let us consider the following multi-dimensional analogue of (1)

$$\frac{\partial u}{\partial t} + \sum_{i=1}^{d} V_i(x_1,\dots,x_d) \frac{\partial f_i(u)}{\partial x_i} = \varepsilon \sum_{i=1}^{d} \frac{\partial^2 u}{\partial x_i^2}. \tag{4}$$

Letting $\mathcal{E}_\Delta^x(t)$ denote our approximate one-dimensional solution (evolution) operator associated with (1), we can then realize the solution of (4) using the product formula

$$u(x_1,\dots,x_d,n\Delta t) \approx \left[\mathcal{E}_\Delta^{x_d}(\Delta t) \circ \cdots \circ \mathcal{E}_\Delta^{x_1}(\Delta t)\right]^n u_0. \tag{5}$$

For scalar hyperbolic equations, combining front tracking and dimensional splitting gives not only a simple, but also an efficient and reliable method, see Lie *et al* (1998). This approach is also attractive for (5) since each $\mathcal{E}_\Delta^{x_i}(t)$ represents an unconditionally stable scheme, which implies that a large time step Δt is feasible, see

§4. In Karlsen *et al* (1998), a Petrov-Galerkin finite element method is employed to solve the diffusion equation instead of the simple finite difference scheme used here. Compared with a standard approach, the results are very promising. By combining the analysis found in §3 with the analysis found in Karlsen & Risebro (1997), it is possible to prove convergence of the multi-dimensional splitting formula (5) (the details will be presented elsewhere).

Our paper is organized as follows. In §2 we describe in detail the front tracking method and the construction of the (corrected) operator splitting solutions. In §3 we establish convergence of these approximate solutions by making use of a L_1 compactness argument. Finally, in §4 we present and discuss some numerical applications of our solution strategy.

2. Construction of Approximate Solutions

The splitting approach results in three different equations that each must be solved numerically. Therefore, before we describe the operator splitting in more detail, we introduce numerical schemes for solving these three equations. But as mentioned earlier, the schemes for the diffusive and the reactive part are deliberately chosen as simple as possible in order to focus on the main ideas of our front tracking/corrected splitting strategy. For less academic purposes, these simple methods obviously *can* and will be replaced by other schemes. Moreover, in some cases it will be feasible to combine the two in a single reaction-diffusion step.

2.1 Advection Equation

In this section, we describe the front tracking method. Consider the nonlinear conservation law

$$v_t + V(x,t)f(v)_x = 0, \qquad v(x,0) = v_0(x), \tag{6}$$

where we assume that $f(v)$ is a continuous piecewise linear function and $v_0(x)$ is a step function with a finite number of jumps. The piecewise constant initial function yields a sequence of Riemann problems of the form

$$v(x,0) = \begin{cases} v_l, & \text{when } x < 0, \\ v_r, & \text{when } x > 0. \end{cases}$$

Each of these Riemann problems can be solved analytically, and, since the flux function f is piecewise linear, the solution will be a step function. Rarefaction waves are replaced by sequences of small shocks. Recall that a discontinuity (v_l, v_r) with associated shock speed $s = (f(v_l) - f(v_r))/(v_l - v_r)$ is admissible provided the entropy condition

$$\operatorname{sgn}(V(x,t)) \left(\frac{f(v) - f(v_r)}{v - v_r} \right) \leqslant \operatorname{sgn}(V(x,t))\, s \leqslant \operatorname{sgn}(V(x,t)) \left(\frac{f(v) - f(v_l)}{v - v_l} \right)$$

is satisfied for all v between v_l and v_r. This condition, which is due to Oleinik (1963), ensures that the solution is physically correct. To give the complete solution of the

Riemann problem, assume first that $V(x,t)$ is positive and introduce the envelope function

$$f_c(v\,;v_l,v_r,V) = \begin{cases} \text{the lower convex envelope of } f \text{ on } [v_l,v_r] \text{ if } v_l < v_r, \\ \text{the upper concave envelope of } f \text{ on } [v_r,v_l] \text{ if } v_l > v_r. \end{cases}$$

For negative $V(x,t)$ the envelope function f_c is defined similarly with the roles of convex and concave interchanged. Suppose that $\{v_i\}$ are the breakpoints of f, i.e., the points where f' is discontinuous. Since f is piecewise linear, then so is f_c, and the breakpoints $\{\bar{v}_i\}$ of f_c form a subset of $\{v_i\}$. If we set $\bar{v}_1 = v_l$ and $\bar{v}_M = v_r$, we can write the solution of the Riemann problem as

$$v(x,t) = \begin{cases} v_l, & x < \bar{x}_0(t), \\ \bar{v}_i, & \bar{x}_i(t) \le x \le \bar{x}_{i+1}(t), \quad i = 1,\ldots,M-1, \\ v_r, & x > \bar{x}_{M-1}(t), \end{cases}$$

where each $\bar{x}_i(t)$ satisfies a Rankine–Hugoniot condition

$$\frac{d\bar{x}_i}{dt} = V(\bar{x}_i,t)\Big(\frac{\bar{f}_{i+1}-\bar{f}_i}{\bar{v}_{i+1}-\bar{v}_i}\Big) = V(\bar{x}_i,t)\bar{s}_i, \tag{7}$$

with $\bar{f}_i = f_c(\bar{v}_i;v_l,v_r)$. The shock paths $\bar{x}_i(t)$ can be computed explicitly if the function $V(x,t)$ has a simple form. For instance, if $V = V(x) = (ax+b)$ with nonzero a, the path of a shock with speed s starting from x_0 at time t_0 is given by $x(t) = (x_0 + b/a)\exp[as(t-t_0)] - b/a$. Connecting the solutions of the local Riemann problems gives the global solution of (6) up to the first time when two waves from neighbouring Riemann problems interact. This interaction defines a new Riemann problem with left and right states given by the values immediately to the left and right of the collision point. The new Riemann problem is then solved as outlined above, thereby, giving the global solution until the next interaction occurs, and so on. Summing up, the front tracking algorithm goes as follows:

(i) Solve the Riemann problems defined by the piecewise constant initial data.
(ii) Keep track of shock collisions and solve Riemann problems at the collision points.

One can prove that the front tracking algorithm is well defined; that is, there are a finite number of shocks and a finite number of shock collisions (even) in infinite time, see Lie (1997). The front tracking method for a general conservation law (arbitrary V, f, and v_0) consists in replacing f with a piecewise linear approximation, v_0 with a piecewise constant approximation, and V by a function on a form such that (7) can be solved explicitly; typically piecewise linear in space and time, which is assumed from now on. Then an approximate solution is found by solving the resulting (perturbed) problem exactly according to the procedure described above. For a more detailed treatment of the front tracking method we refer to Lie (1997).

2.2 Diffusion Equation

As pointed out earlier, diffusion is modelled by realizing an equation of the form

$$w_t = \varepsilon w_{xx}, \qquad w(x,0) = w_0(x),$$

where we assume that the data $w_0(x)$ is of bounded variation. When integrating this kind of parabolic equations, one can choose from a diversity of numerical schemes. Here we will simply employ an explicit finite difference scheme. Let h and k be the spatial and temporal increments; that is, $x_i = ih$ and $t_m = mk$ for $i \in \mathbb{Z}$ and $m \in \mathbb{Z}_+$. We assume that the stability condition $\alpha \equiv \varepsilon k/h^2 \leq 1/2$ is satisfied. The approximation to $w(x_i, t_m)$ will be denoted by w_i^m. To start the scheme we set $w_i^0 = (\pi w_0)(x_i)$, where π denotes the usual grid cell averaging operator on $\{x_i; h\}$. We compute w_i^{m+1} from the finite difference equation

$$w_i^{m+1} = \alpha w_{i-1}^m + (1-2\alpha) w_i^m + \alpha w_{i+1}^m, \qquad (i,n) \in \mathbb{Z} \times \mathbb{Z}_+. \tag{8}$$

For later use, we introduce the interpolation $w_\Delta(x,t) = w_i^m$ for $(x,t) \in [x_i, x_{i+1}\rangle \times [t_m, t_{m+1}\rangle$.

2.3 Reaction Equation

To realize reactive/source/sink processes we use the forward–Euler method to solve an ordinary differential equation of the form

$$z_t = Q(x,t,z), \qquad z(x,0) = z_0(x).$$

To start the scheme we set $z_i^0 = z_0(x_i)$ and then compute z_i^{m+1} from z_i^m using the equation

$$z_i^{m+1} = z_i^m + kQ_i^m, \qquad (i,n) \in \mathbb{Z} \times \mathbb{Z}_+, \qquad Q_i^m = Q(x_i, t_m, z_i^m). \tag{9}$$

For later use, introduce the interpolation $z_\Delta(x,t) = z_i^m$ for $(x,t) \in [x_i, x_{i+1}\rangle \times [t_m, t_{m+1}\rangle$.

2.4 Splitting Algorithm

From now on, let $h > 0$ and $\Delta t > 0$ denote the spatial and temporal discretization parameters, i.e., $x_i = ih$ for $i \in \mathbb{Z}$ and $t_n = n\Delta t$ where $n \leqslant N$ and $N\Delta t = T$. Define $V^\Delta(x,t)$ and $f^\delta(u)$ to be proper piecewise linear approximations to $V(x,t)$ and $f(u)$, respectively ($\delta > 0$ denotes a polygonal approximation parameter). Here, and in the following, Δ will indicate several discretization parameters which we choose not to specify. Assume that we know the approximate solution u^n at time $t = t_n$, for some fixed $n < N$. Next, we describe how to construct u^{n+1} from u^n.

Step 1 (advection): Let $v(x,t) = \mathcal{S}_\Delta(t)u^n$ be the front tracking solution to the conservation law

$$v_t + V^\Delta(x,t) f^\delta(v)_x = 0, \qquad v(x,0) = u^n(x), \qquad (x,t) \in \mathbb{R} \times \langle 0, \Delta t], \tag{10}$$

and introduce the intermediate solution $u^{n+1/3} = \mathcal{S}_\Delta(\Delta t)u^n$.

Step 2 (diffusion): Choose a local time step k_d such that $k_d N_d = \Delta t$ and $\alpha_d = \varepsilon k_d/h^2 \leq 1/2$. Let $w_\Delta(x,t) = \mathcal{H}_\Delta(t)u^{n+1/3}$ be the finite difference solution of the parabolic problem

$$w_t = \varepsilon w_{xx}, \qquad w(x,0) = u^{n+1/3}(x), \qquad (x,t) \in \mathbb{R} \times \langle 0, \Delta t]. \tag{11}$$

Then introduce the intermediate solution $u_-^{n+2/3} = \mathcal{H}_\Delta(\Delta t)u^{n+1/3}$.

As pointed out earlier, it can be necessary to do a correction step to get the structure of steep fronts right. To this end, recall that the function $u^{n+1/3}(x)$ is piecewise constant on a finite number of intervals given by $\{y_i\}$. Let $\{\tilde{u}_i\}$ denote the values that $u^{n+1/3}$ takes; that is, $\tilde{u}_i$ and $\tilde{u}_{i+1}$ denote the left and right limits, respectively, of $u^{n+1/3}$ at the discontinuity point $x = y_i$. Choose positions $\{\bar{x}_i\}$ such that y_i is located somewhere in the interval $\langle \bar{x}_i, \bar{x}_{i+1}\rangle$. Then define the residual flux function (suppressing dependency on n) by

$$f_{\mathrm{res}}^{\delta}(x,u) = \begin{cases} f^{\delta}(u) - f_c^{\delta}(u;\tilde{u}_i,\tilde{u}_{i+1},V^{\Delta}), & x \in [\bar{x}_i,\bar{x}_{i+1}\rangle,\ u \in [\tilde{u}_i,\tilde{u}_{i+1}], \\ 0, & x \in [\bar{x}_i,\bar{x}_{i+1}\rangle,\ u \notin [\tilde{u}_i,\tilde{u}_{i+1}]. \end{cases} \tag{12}$$

Introduce a small positive parameter τ, later referred to as the correction time, and let $v_i(x,t)$ denote the front tracking solution to the (local) residual conservation law

$$\frac{\partial v_i}{\partial t} + V^{\Delta}(x,t)\frac{\partial f_{\mathrm{res}}^{\delta,i}(v_i)}{\partial x} = 0, \qquad (x,t) \in [\bar{x}_i,\bar{x}_{i+1}\rangle \times \langle 0,\tau], \tag{13}$$

with data $v_i|_{t=0} = u_-^{n+2/3}$ restricted to $[\bar{x}_i,\bar{x}_{i+1}\rangle$. Here $f_{\mathrm{res}}^{\delta,i}$ denotes the residual flux function $f_{\mathrm{res}}^{\delta}$ restricted to the interval $[\bar{x}_i,\bar{x}_{i+1}\rangle$. Connect the solutions of (13) for all i and let $v(x,t)$ denote this solution (defined for all $x \in \mathbb{R}$). Moreover, let $\mathcal{C}(t)$ denote the associated solution operator. We then define $u^{n+2/3} = \mathcal{P}_{\Delta,\tau}(\Delta t)u^{n+1/3}$, where $\mathcal{P}_{\Delta,\tau}(t)$ is the compound operator $\mathcal{C}(\tau)\circ\mathcal{H}_\Delta(t)$.

Step 3 (reaction/source/sink): Let $z_\Delta(x,t) = \mathcal{R}_\Delta(t)u^{n+2/3}$ be the solution of

$$z_t = Q(x,z), \qquad z(x,0) = u^{n+2/3}(x), \qquad (x,t) \in \mathbb{R}\times\langle 0,\Delta t] \tag{14}$$

computed by the forward–Euler scheme using N_r time steps of length k_r, i.e, $N_r k_r = \Delta t$. Finally, define the splitting solution at time $t = t_{n+1}$ by $u^{n+1} = \mathcal{R}_\Delta(\Delta t)u^{n+2/3}$.

The splitting solution $\{u^n\}_{n=0}^N$ is constructed inductively. First, set $u^0 = \pi u_0$ and then compute u^{n+1} from u^n for all $0 \leqslant n < N$ using the product formula

$$u^{n+1} = \big[\mathcal{R}_\Delta(\Delta t)\circ\mathcal{P}_{\Delta,\tau}(\Delta t)\circ\mathcal{S}_\Delta(\Delta t)\big]u^n. \tag{15}$$

3. Convergence

It is well known that there exists a unique classical solution $u(x,t)$ to the initial-value problem (1). For $t > 0$ the solution has all the continuous derivatives occurring in the equation. Furthermore, the initial data is in general assumed in the weak sense, i.e.,

$$\int \big(u(x,t) - u_0(x)\big)\phi(x)\,dx \to 0, \qquad t \to 0+, \qquad \forall \phi \in C_0(\mathbb{R}).$$

We recall that a function $u(x,t)$ is called a weak or generalized solution to (1) provided

$$\iint \Big(u\phi_t + F(x,t,u)\phi_x + \varepsilon u\phi_{xx} - G(x,t,u)\phi\Big)\,dt\,dx + \int u_0\phi\big|_{t=0}\,dx = 0, \tag{16}$$

for all test functions $\phi \in C_0^\infty(Q_T)$ with $\phi|_{t=T} \equiv 0$. Moreover, the weak solution $u(x,t)$ is unique and possesses for $t > 0$ all the continuous derivatives occurring in (1) and satisfies this equation. Consequently, the notion of classical and weak solutions coincide. All these claims are rigorously proved by Oleinik (1963).

We will now show that a sequence of splitting solutions is compact in the L_1 topology. For simplicity we first assume that the residual term f_{res} is zero, and then towards the end of this section discuss the case with a nonzero residual flux term. The splitting scheme in our analysis then takes the form

$$u^{n+1} = \left[\mathcal{R}_\Delta(\Delta t) \circ \mathcal{H}_\Delta(\Delta t) \circ \mathcal{S}_\Delta(\Delta t)\right] u^n. \tag{17}$$

By making appropriate assumptions (see Theorem 3.1) on $V(x,t)$, $f(u)$, and $G(x,t,u)$, we obtain the following bounds on the source term $Q(x,t,u) = G(x,t,u) - f(u)V_x(x,t)$:

$$|Q(x,t,u)| \le Q_\infty, \qquad TV\left(Q(\cdot,t,u)\right) \le Q_V, \qquad \|Q(x,t,\cdot)\|_{\text{Lip}} \le Q_L, \tag{18}$$

where Q_∞, Q_v, and Q_L are finite constants independent of x, t, and u. The above bounds need only hold locally with respect to the third argument, due to the maximum principle for equations of the form (1). We shall in what follows assume (for convenience) that $h = \mathcal{O}(1)\Delta t$.

LEMMA 3.1 The splitting solution u^n is bounded; that is, $\|u^n\|_\infty \leqslant M_1(T)$ for some constant $M_1(T)$ independent of the discretization parameters and n.

Proof. Fix an integer $l < n$. By construction we know that the solution operator $\mathcal{S}_\Delta(t)$ does not introduce new extrema and neither does $\mathcal{H}_\Delta(t)$. The latter is true due to the convex nature of the finite difference scheme (8) and because π is the simple grid cell averaging operator. Furthermore, (9) gives that $\|z^{m+1}\|_\infty \leqslant \|z^m\|_\infty + k_r Q_\infty$, for each $m \leqslant N_r$. Induction on m and l implies that $\|u^n\|_\infty \leqslant \|u_0\|_\infty + n\Delta t Q_\infty \le M_1(T)$. □

LEMMA 3.2 The total variation of the splitting solution u^n is finite; that is, $TV\,(u^n) \leqslant M_2(T)$ for some constant $M_2(T)$ independent of the discretization parameters and n.

Proof. Fix an integer $l < n$. Let us first consider the front tracking operator $\mathcal{S}_\Delta(t)$. The variation only changes when shock fronts (discontinuity lines) from neighbouring Riemann problems collide. Suppose that two or more fronts collide and let $u_1,\ldots,u_K$ be the values that meet in the collision. After the collision, there will be at least one new shock front, unless the values u_1 and u_K are equal. When $u_1 = u_K$, all the intermediate values disappear and the total variation decreases in the collision. If the collision produces new shocks, u_1 will be the value to the left of the leftmost shock and u_K the value to the right of the rightmost shock, and the values in between will form a monotone sequence. Accordingly, all of the values $u_2,\ldots,u_{K-1}$ that are not between u_1 and u_K disappear and the total variation decreases. Consequently, we can conclude that $TV\left(\mathcal{S}_\Delta(\Delta t)u^l\right) \le TV\left(u^l\right)$.

The operator π does not increase the total variation. By using the convex nature

of (8), it easily follows that $TV\left(\mathcal{H}_\Delta(\Delta t)u^{l+1/3}\right) \leqslant TV\left(u^{l+1/3}\right)$. Let us finally look at the reaction operator $\mathcal{R}_\Delta(t)$. Fix an integer $m < N_r$. We then readily get

$$\begin{aligned}\sum_i \left|z_{i+1}^{m+1} - z_i^{m+1}\right| &\leqslant \sum_i \left|z_{i+1}^m - z_i^m\right| \\ &+k_r \sum_i \left|Q(x_{i+1}, t_m, z_{i+1}^m) - Q(x_i, t_m, z_{i+1}^m)\right| \\ &+k_r \sum_i \left|Q(x_i, t_m, z_{i+1}^m) - Q(x_i, t_m, z_i^m)\right|.\end{aligned}$$

This implies that $TV\left(z^{m+1}\right) \leqslant (1+k_rQ_L)TV\left(z^m\right) + k_rQ_V$ and can be further expanded as $TV\left(z^{m+1}\right) \leq (1+k_rQ_L)^m TV\left(z^0\right) + mk_rQ_V(1+k_rQ_L)^m$. Consequently, the splitting solution $u^{l+1} = \mathcal{R}_\Delta(\Delta t)u^{l+2/3}$ at time level $t = (l+1)\Delta t$ satisfies

$$TV\left(u^{l+1}\right) \leqslant e^{\Delta t Q_L} TV\left(u^{l+2/3}\right) + \Delta t e^{\Delta t Q_L} Q_V \leq e^{\Delta t Q_L} TV\left(u^l\right) + \Delta t e^{\Delta t Q_L} Q_V.$$

By induction on l we get $TV\left(u^n\right) \leqslant e^{n\Delta t Q_L} TV\left(u_0\right) + n\Delta t e^{n\Delta t Q_L} Q_V \leq M_2(T)$. □

LEMMA 3.3 The splitting solution u^n is L_1 Hölder continuous in the time variable with exponent $1/2$; that is, $\|u^p - u^q\|_1 \leqslant M_3(T)\sqrt{|(p-q)\Delta t|}$ for some constant $M_3(T)$ independent of the discretization parameters and q, p.

Proof. Fix an integer l between q and p, for $q < p$. Since all waves in the front tracking solution have finite speed of propagation and the total variation is finite, it follows that $\|\mathcal{S}_\Delta(\Delta t)u^l - u^l\|_1 = \mathcal{O}(1)\Delta t$. Moreover, using (18) it is easy to see that the reaction operator $\mathcal{R}_\Delta(t)$ obeys the bound $\|\mathcal{R}_\Delta(\Delta t)u^{l+2/3} - u^{l+2/3}\|_1 = \mathcal{O}(1)\Delta t$. It is well known that the solution of the difference equation (8), with BV initial data, is merely L_1 Hölder continuous in time with exponent $1/2$ (consult Section 2 in Hoff & Smoller (1985)). Therefore, we first need to establish a weak Lipschitz continuity result of the finite difference solution. To this end, let $\phi(x)$ be a test function (with compact support) and $\phi_h(x)$ its piecewise constant approximation; $\phi_h(x) = \sum_i \phi_i \chi_{[x_i, x_{i+1}]}(x)$, where $\phi_i = \phi(x_i)$. Using the difference equation (8) and summation by parts, we get

$$\begin{aligned}\left|\sum_i \phi_i\big(w_i^{N_d} - w_i^0\big)h\right| &= \left|\sum_{m,i} \phi_i\big(w_i^{m+1} - w_i^m\big)h\right| \\ &= \left|\sum_{m,i} h\phi_i\left[\alpha_d(w_{i-1}^m - 2w_i^m + w_{i+1}^m)\right]\right| \\ &= \alpha_d h\left|\sum_{m,i} \phi_i\big(w_{i-1}^m - 2w_i^m + w_{i+1}^m\big)\right| = \alpha_d h\left|\sum_{m,i} (\phi_{i+1} - \phi_i)\big(w_{i+1}^m - w_i^m\big)\right| \\ &\leqslant \alpha_d h^2 N_d \|\phi_x\|_\infty \sup_m \sum_i \left|w_{i+1}^m - w_i^m\right| = \mathcal{O}(1)\Delta t\|\phi_x\|_\infty,\end{aligned}$$

where we also have used Lemma 3.2. From this inequality, we get the weak estimate (recall that $h = \mathcal{O}(1)\Delta t$)

$$\left|\int \phi\big(\mathcal{H}_\Delta(\Delta t)u^{l+1/3} - u^{l+1/3}\big)\,dx\right| \leq \left|\int \phi_h\big(\mathcal{H}_\Delta(\Delta t)u^{l+1/3} - u^{l+1/3}\big)\,dx\right|$$

$$
\begin{aligned}
&+\Big|\int(\phi-\phi_h)\big(\mathcal{H}_\Delta(\Delta t)u^{l+1/3}-u^{l+1/3}\big)\,dx\Big| \\
\leq\ & \Big|\sum_i \phi_i\big(w_i^{N_d}-w_i^0\big)h\Big| + \mathcal{O}(1)h\|\phi\|_\infty + h\|\phi_x\|_\infty\|\mathcal{H}_\Delta(\Delta t)u^{l+1/3}-u^{l+1/3}\|_1 \\
=\ & \mathcal{O}(1)\Delta t\big(\|\phi\|_\infty+\|\phi_x\|_\infty\big)+\mathcal{O}(1)\|\phi_x\|_\infty\Delta t = \mathcal{O}(1)\Delta t\big(\|\phi\|_\infty+\|\phi_x\|_\infty\big).
\end{aligned}
$$

We thus conclude that

$$
\Big|\int\phi\big(u^p-u^q\big)\,dx\Big| = \mathcal{O}(1)(p-q)\Delta t\big(\|\phi\|_\infty+\|\phi_x\|_\infty\big).
$$

This weak estimate can now be interpolated into a strong L_1 Hölder estimate with exponent $1/2$ along the lines of Karlsen & Risebro (1997). This concludes the proof of the lemma. □

Now we need to consider functions defined in the interval $\langle 0,T]$, and not merely on the time-strips $t=t_n$. To accomplish this, define the sequence $\{u_\Delta\}$ by

$$
u_\Delta(x,t) = \begin{cases} \mathcal{S}_\Delta\big(2(t-t_n)\big)\,u^n, & t\in\langle t_n, t_{n+1/2}\rangle, \\ \mathcal{H}_\Delta\big(2(t-t_{n+1/2})\big)\,u^{n+1/3}, & t\in[t_{n+1/2}, t_{n+1}\rangle, \\ \mathcal{R}_\Delta(\Delta t)u^{n+2/3}, & t=t_{n+1}, \end{cases} \tag{19}
$$

where $u^{n+1/3}$ and $u^{n+2/3}$ are as defined above. Note that $u_\Delta(x,t_n)=u^n$ for all n. This method of extending u^n to a function defined for all $t>0$ is motivated by Crandall & Majda (1980) and Karlsen & Risebro (1997). In view of the previous lemmas, we conclude that there exists a finite constant $M=M(T)$ (independent of Δ) such that $u_\Delta(x,t)$ obeys:

$$
\|u_\Delta(\cdot,t)\|_\infty \leqslant M, \quad TV\,(u_\Delta(\cdot,t)) \leqslant M, \quad \|u_\Delta(\cdot,t_2)-u_\Delta(x,t_1)\|_1 \leqslant M\sqrt{|t_2-t_1|}.
$$

Now a standard application of Helly's theorem (see Oleinik (1963)) yields the desired $L_1^{\mathrm{loc}}(Q_T)$ convergence of a subsequence, still denoted by $\{u_\Delta\}$, to a limit function u. We finally justify the term "approximate solution" by proving that $u(x,t)$ is the (classical) solution of (1).

LEMMA 3.4 The limit $u(x,t)$ is the classical solution of the Cauchy problem (1).

Proof. Let $\mathcal{L}_\phi(u)$ denote the left-hand side of (16). It then suffices to prove that $\mathcal{L}_\phi(u)=0$ for all proper test functions ϕ with $\phi|_{t=T}=0$. To this end, let $v_n(t)=\mathcal{S}_\Delta(t)u^n$, $t\in\langle 0,\Delta t]$, and define a new test function φ by $\varphi(x,t)=\phi(x,t/2)$. Then, since $v_n(t)$ is an exact solution to the (perturbed) conservation law (10), the following equality holds

$$
\begin{aligned}
&\int\int_{t_n}^{t_{n+1/2}}\Big(\frac{1}{2}u_\Delta\phi_t + f^\delta(u_\Delta)\big(V^\Delta(x,t)\phi\big)_x\Big)\,dt\,dx \\
&\qquad = \frac{1}{2}\int\int_0^{\Delta t}\Big(v_n(\xi)\varphi_\tau + f^\delta(v_n(\xi))\big(V^\Delta(x,\xi)\phi\big)_x\Big)\,d\xi\,dx \qquad (20)\\
&\qquad = \frac{1}{2}\int u^{n+1/3}\phi\big|_{t=t_{n+1/2}}\,dx - \frac{1}{2}\int u^n\phi\big|_{t=t_n}\,dx,
\end{aligned}
$$

where we have used the substitution $\xi = 2(t - t_n)$. Let $\{t_m\}$ denote the local time levels associated with the time step k_d and let $\phi_i^m = \phi(x_i, t_m)$. Multiplying the finite difference equation (8) by $\phi_i^m k_d h$ and applying summation by parts, we get

$$\begin{aligned} k_d h \sum_i \sum_m w_i^m \Big[\frac{\phi_i^{m+1} - \phi_i^m}{k_d}\Big] + k_d h \sum_i \sum_m \varepsilon w_i^m \Big[\frac{\phi_{i-1}^m - 2\phi_i^m + \phi_{i+1}^m}{h^2}\Big] \\ = \sum_i w_i^{N_d} \phi_i^{N_d} h - \sum_i w_i^0 \phi_i^0 h, \qquad w_i^0 = (\pi u^{n+1/3})(x_i). \end{aligned}$$

Letting $w_\Delta(x,t) = \mathcal{H}_\Delta(\Delta t) u^{n+1/3}$, we can obviously replace this equality by

$$\begin{aligned} \int\int_0^{\Delta t} \Big(w_\Delta \phi_t + \varepsilon w_\Delta \phi_{xx} \Big)\, dt\, dx = \\ \int u^{n+2/3} \phi\big|_{t=\Delta t}\, dx - \int u^{n+1/3} \phi\big|_{t=0}\, dx + \int \big(u^{n+1/3} - \pi u^{n+1/3}\big)\phi\big|_{t=0}\, dx, \end{aligned}$$

making an allowable error of order $\mathcal{O}(1)(\Delta t h + \Delta t k_d) = \mathcal{O}(1)\Delta t^2$. Within an allowable error of order $\mathcal{O}(1)\Delta t^2$, we then deduce that

$$\begin{aligned} \int\int_{t_{n+1/2}}^{t_{n+1}} \Big(\frac{1}{2} u_\Delta \phi_t + \varepsilon u_\Delta \phi_{xx} \Big)\, dt\, dx = \\ \frac{1}{2} \int (u_\Delta \phi)\big|_{t=t_{n+1}^-} dx - \frac{1}{2} \int u^{n+1/3} \phi\big|_{t=t_{n+1/2}} dx \\ + \frac{1}{2} \int \big(u^{n+1/3} - \pi u^{n+1/3}\big)\phi\big|_{t=t_{n+1/2}} dx. \end{aligned}$$

Having in mind (9) and (18), a straightforward calculation yields

$$\int (u_\Delta \phi)\big|_{t=t_{n+1}^-} dx = \int u^{n+1} \phi\big|_{t=t_{n+1}} dx - \int\int_{t_n}^{t_{n+1}} Q(x,t,u_\Delta)\phi\, dt\, dx$$

within an allowable error of order $\mathcal{O}(1)\Delta t^{3/2}$. If we now add the approximate weak formulations for $u_\Delta(x,t)$ on $\langle t_n, t_{n+1/2}\rangle$ and $\langle t_{n+1/2}, t_{n+1}]$, and sum over n, the resulting global weak formulation takes the form

$$\begin{aligned} \sum_{n=0}^{N-1} \int\int_{t_n}^{t_{n+1}} \Big(\frac{1}{2} u_\Delta \phi_t + \chi_n(t) f^\delta(u_\Delta) \big(\phi V^\Delta(x,t)\big)_x + (1 - \chi_n(t)) \varepsilon u_\Delta \phi_{xx} \\ + \frac{1}{2} Q(x,t,u_\Delta)\phi \Big)\, dt\, dx + \frac{1}{2} \int u_0 \phi\big|_{t=0}\, dx \qquad (21) \\ = \frac{1}{2} \sum_{n=0}^{N-1} \int \Big(u^{n+1/3} - \pi u^{n+1/3} \Big) \phi\big|_{t=t_{n+1/3}}\, dx + \mathcal{O}(1)\sqrt{\Delta t}, \end{aligned}$$

where $\chi_n(t)$ denotes the characteristic function of the interval $\langle n\Delta t, (n+1/2)\Delta t\rangle$. Note that $\chi_n(t)$ tends weakly in L_2 to $1/2$. We assume that f^δ and V^Δ are chosen such that $\|f - f^\delta\|_{W^{1,\infty}} \to 0$ and $\|V - V^\Delta\|_{W^{1,\infty}} \to 0$ as $\Delta \to 0$. Furthermore, the

global projection error (the right-hand side of the equality (21)) tends to zero as $\Delta \to 0$, see Karlsen & Risebro. In view of the dominated convergence theorem, we can thus pass to the limit as $\Delta \to 0$ in (21), obtaining (remember that $Q = G - fV_x$)

$$\mathcal{L}_\phi(u) = \lim_{\Delta \to 0} \mathcal{L}_\phi(u_\Delta) = 0,$$

where $u = \lim_{\Delta \to 0} u_\Delta$ in $L_1^{\mathrm{loc}}(Q_T)$. This concludes the proof of the lemma. □

Consequently, we have the following main theorem.

THEOREM 3.1 Let $F(x,t,u) = V(x,t)f(u)$ be the flux term and $G(x,t,u)$ the reaction term. Suppose that V, f, and G are bounded and smooth functions of all their arguments. In addition, suppose that $G(\cdot,t,u)$ and $V_x(\cdot,t)$ have bounded variation and that the initial data u_0 is a function of bounded variation. Then the operator splitting solutions (19) converge in $L_1^{\mathrm{loc}}(Q_T)$ to the unique classical solution of the Cauchy problem

$$\frac{\partial u}{\partial t} + \frac{\partial F(x,t,u)}{\partial x} = \varepsilon \frac{\partial^2 u}{\partial x^2} + G(x,t,u), \qquad u(x,0) = u_0(x), \qquad (x,t) \in Q_T.$$

REMARK 3.1 The convergence argument used to prove Theorem 3.1 is a compactness argument often used in the context of nonlinear hyperbolic conservation laws. The advantage with this 'hyperbolic approach' is that the estimates we obtain are independent of the (small) scaling parameter ε, see Lemmas 3.1–3.3. This fact is in strong contrast to the estimates one obtains with more traditional parabolic (energy) arguments. However, we do not obtain error estimates with our approach. But, independently of the method of analysis, we believe that it is a *highly* nontrivial matter to derive *rigorous* error estimates for our operator splitting method. One reason for this claim is that the advection solver will, in general, produce non-smooth (discontinuous) functions, which in turn are used as initial data for the diffusion solver. However, for smooth (hyperbolic) solutions, an application of Strang's result (Strang (1968)) gives first order convergence when using exact solution operators. Smooth solutions can be ensured provided the time step is chosen sufficiently small. Similarly, second order convergence follows by using Strang splitting (Strang (1968)).

REMARK 3.2 It should be noted that if we use an implicit diffusion solver, our operator splitting method is unconditionally stable in the sense that the time step Δt is not limited by the space discretization Δx, i.e., no CFL condition is associated with the method. Hence, whenever the physics of the problem allows for it, large time steps can be used.

Let us now consider the corrected splitting formulas (15). Introduce the slightly modified interpolation $u_{\Delta,\tau}(x,t)$,

$$u_{\Delta,\tau}(x,t) = \begin{cases} \mathcal{S}_\Delta\big(2(t-t_n)\big)u^n, & t \in \langle t_n, t_{n+1/2}\rangle, \\ \mathcal{H}_\Delta\big(2(t-t_{n+1/2})\big)u^{n+1/3}, & t \in [t_{n+1/2}, t_{n+1}\rangle, \\ \mathcal{R}_\Delta(\Delta t) \circ \mathcal{C}(\tau) u_-^{n+2/3}, & t = t_{n+1}, \end{cases} \qquad (22)$$

where we assume that $\tau = \mathcal{O}(1)\Delta t$. Lemmas 3.1–3.3 are still valid (the operators

$\mathcal{S}_\Delta(t)$ and $\mathcal{C}(\tau)$ have similar properties). Thus the sequence $\{u_{\Delta,\tau}(x,t)\}$ is compact in $L_1^{loc}(Q_T)$. In view of Lemma 3.4, we get that $u_{\Delta,\tau}(x,t)$ satisfies the weak formulation (21) with the extra "error" term

$$\begin{aligned}\sum_{n=0}^{N-1}\int\Big(\mathcal{C}(\tau)u_-^{n+2/3}-u_-^{n+2/3}\Big)\phi(x,t_{n+1})\,dx\\ =\sum_{n=0}^{N-1}\int_0^\tau\sum_i\int_{\bar{x}_i}^{\bar{x}_{i+1}}\big(V^\Delta\phi(x,t_{n+1})\big)\frac{\partial f_{\mathrm{res}}^{\delta,i}}{\partial x}(v_i)\,dx\,dt,\end{aligned}\tag{23}$$

where $v_i(x,t)$ is the solution of (13), which is for the moment assumed to be smooth. First, suppose that there is only one residual flux term. For notational convenience we name it g and let $v(x,t)$ denote the solution of the corresponding residual conservation law (13), which is defined on $\mathbb{R}\times\langle 0,\tau]$. Recall that $v(x,t)$ depends on n and the discretization parameters Δ. Let $\phi\in C_0^\infty(\mathbb{R})$ and put $\Phi(x,t)=V^\Delta(x,t)\phi(x,t_{n+1})$. Observe first that $g(v)$ has finite total variation because of Lemma 3.2, and that Φ_x is uniformly bounded independently of Δ and τ. Using integration by parts we get

$$\begin{aligned}\Big|\int\Phi(x)\frac{\partial}{\partial x}g(v)\,dx\Big| &\le \Big\|\frac{\partial\Phi}{\partial x}\Big\|_\infty\int|g(v)|\,dx=\mathcal{O}(1)\int\big|g(v)-g\big(u^{n+1/3}\big)\big|\,dx\\ &= \mathcal{O}(1)\int\big|v(x,t)-u^{n+1/3}(x)\big|\,dx=\mathcal{O}(1)\sqrt{\Delta t},\end{aligned}\tag{24}$$

where we have also used the key property $g(u^{n+1/3})\equiv 0$ for all n, the Lipschitz continuity of g, and Lemma 3.3.

Let us now briefly comment on the case with several residual flux terms. Let $v_i(x,t)$ be the solution of (13) with residual flux function g_i. We stress that in "worst case" scenarios the operator $\mathcal{H}_\Delta(\Delta t)$ can destroy significant structures of $u^{n+1/3}$ (e.g. monotonicity properties and local extrema), so that $\mathcal{C}(\tau)$ possesses no correction effect when applied to $u^{n+2/3}$. We will therefore apply the correction operator on an interval $[\bar{x}_i,\bar{x}_{i+1}\rangle$ only if the following two conditions are fulfilled. First, we require that

$$\begin{aligned}\operatorname{sgn}(V^\Delta(\bar{x}_i,t))g_i'\big(u^{n+2/3}(\bar{x}_i)\big)\ge 0,\\ \operatorname{sgn}(V^\Delta(\bar{x}_{i+1},t))g_i'\big(u^{n+2/3}(\bar{x}_{i+1})\big)\le 0.\end{aligned}\tag{25}$$

Note that (25) is necessary for the conservation law (13) to actually possess a correction effect on $u^{n+2/3}$. Consequently, on intervals $\langle\bar{x}_i,\bar{x}_{i+1}\rangle$ where (25) is violated, the correction operator operator is not applied since it would not have a correction effect there. Secondly, we require the relation

$$\big|u_-^{n+2/3}(\bar{x}_i)-u^{n+1/3}(\bar{x}_i)\big|\le C\sqrt{\Delta t},\tag{26}$$

where C is a finite constant independent of the discretization parameters and the position $\bar{x}_i$, but dependent on the initial data and the flux function. This condition

is, however, merely a technical assumption associated with the convergence analysis. The assumptions (25) and (26) imply that the following relation holds

$$\left|v_i(\bar{x}_i,t)-\tilde{u}_i\right| = \mathcal{O}(1)\sqrt{\Delta t}. \tag{27}$$

The argument leading to (24) can now be applied to each of the integrals on the right-hand side of the equality (23). The result coincides with (24) except for additional boundary terms (due to integration by parts) of the form

$$\begin{aligned} BT_i &= V^{\Delta}(\bar{x}_{i+1},t)g_i(v_i(\bar{x}_{i+1},t))\phi(\bar{x}_{i+1},t_{n+1}) \\ &\quad -V^{\Delta}(\bar{x}_i,t)g_i(v_i(\bar{x}_i,t))\phi(\bar{x}_i,t_{n+1}). \end{aligned} \tag{28}$$

Using the property $g_i(\tilde{u}_i) = g_i(\tilde{u}_{i+1}) = 0$, the Lipschitz continuity of g_i and the relation (27), we get that $\left|BT_i\right| = \mathcal{O}(1)\sqrt{\Delta t}$. By summing over all i, we obtain that

$$\sum_{n=0}^{N-1}\int\left(\mathcal{C}(\tau)u_-^{n+2/3}-u_-^{n+2/3}\right)\phi(x,t_{n+1})\,dx = \mathcal{O}(1)\sqrt{\Delta t}. \tag{29}$$

The arguments leading to this estimate have been formal (v_i was assumed to be smooth), but they can be made rigorous by using a standard approximation argument (smoothing by convolution). Since this argument is very similar to the one used in Karlsen & Risebro, we omit the details. Equipped with (29), our second main theorem now follows easily.

THEOREM 3.2 In addition to the hypotheses of Theorem 3.1, assume that the correction operator $\mathcal{C}(\tau)$, $\tau = \mathcal{O}(1)\Delta t$, is only applied where (25) and (26) are fulfilled. Then the conclusion of Theorem 3.1 is also valid for the corrected operator splitting solutions (22).

Of course, the above convergence theorems are also true for equations that are in non-conservative form to begin with, i.e., equations of the form

$$u_t + V(x,t)f(u)_x = \varepsilon u_{xx} + G(x,t,u).$$

4. Numerical Examples

In this section we present four numerical examples. The first example discusses the performance of the splitting methods near sharp fronts and demonstrates the effect of correction. In the second example we compare the method with a finite difference scheme to indicate the efficiency of the operator splitting methods. The third example is a convergence study that confirms first order convergence. Finally, the fourth example gives an application to modelling of glacier movement and growth.

However, let us first make a detour and discuss the correction strategy in some more detail. First, a few words on the implementation of the correction step. Although the residual term is defined for every discontinuity in the advection solution, it is zero for all steps of size δ (i.e., rarefaction waves). Similarly, it has little effect for "small" discontinuities. To increase code efficiency, we introduce a threshold

that the strength of a shock in the advection solution must exceed before the corresponding residual flux term is computed. We stress that the conditions (25) and (26) therefore have no practical consequences.

Moreover, instead of having a separate correction step, the residual flux term can be included in the equation modelling diffusion. We then get the following parabolic equation

$$w_t + V^\Delta(x,t) f^\delta_{\mathrm{res}}(x,w)_x = \varepsilon w_x, \qquad (x,t) \in \mathbb{R} \times \langle 0, \Delta t], \tag{30}$$

which must be solved with data $w|_{t=0} = u^{n+1/3}$. It is not difficult to modify the difference scheme (8) so that it takes into account the residual term f^δ_{res}. To this end, consider a fixed interval $\langle \bar{x}_i, \bar{x}_{i+1} \rangle$ on which f^δ_{res} is nonzero (on intervals where f^δ_{res} is zero, the scheme is not altered). Let g_i denote this residual term. Restricted to the ith interval, we compute the solution according to the following modified difference formula

$$w_j^{m+1} = -\beta_d V^\Delta(x_j, t_m)\big(g^m_{i,j+1} - g^m_{i,j-1}\big) + \alpha_d w^m_{j-1} + (1-2\alpha_d) w^m_j + \alpha_d w^m_{j+1}, \tag{31}$$

for all j such that $x_j \in \langle \bar{x}_i, \bar{x}_{i+1} \rangle$. Here $\beta_d = k_d/(2h)$ and $g^n_i = g_i(w^n_j)$. Recall that (31) is stable provided $\alpha_d = \varepsilon k_d / h^2 \le 1/2$ and $h \max(|V^\Delta|\,|g_i'|) \le 2\varepsilon$. Consult Hoff & Smoller (1985) for a discussion of this scheme when $V^\Delta = 1$. In applications, a more sophisticated scheme may be used; we have for instance successfully applied a Petrov–Galerkin finite element method instead of (31), see Karlsen *et al* (1998). The advantage with (30) is that we avoid choosing the parameter τ, but at the expense of solving a more complicated diffusion equation.

Henceforth, OS will refer to the splitting (17) and COS to the corrected version. We will refer to the COS method with a separate correction step as COS(sc), while COS(md) denotes the method with a modified diffusion equation. Note that in most plots below, approximate solutions are deliberately plotted as piecewise constants.

4.1 Example 1

In the first example we demonstrate that OS gives too wide representation of steep fronts if the time step is chosen too large, whereas COS will produce the correct balance between advection and diffusion for any time step. Therefore, consider

$$u_t + \big(1 + 3\sin(\pi x)/4\big)\big[4u^2(1-u^2)\big]_x = \varepsilon u_{xx}, \qquad x \in [-2,2],\ t > 0,$$

with Riemann initial data $u_0(x) = -\mathrm{sgn}(x)$.

Figure 1 shows the approximate solutions at time $t = 0{\cdot}3$ for $\varepsilon = 0{\cdot}1$ computed using OS and COS with one time step. Since the time step is only slightly larger than the diffusion scale, OS gives only a moderate smearing of the front. This temporal splitting error is reduced in both COS schemes. Notice that the approximation in all three runs overshoots the solution in the continuous region to the left of the steep front, and undershoots to the right. In Figure 2 we have zoomed in on the approximations around the steep front. The left plot in Figure 3 shows the residual flux used by both COS methods in a similar run with $\varepsilon = 0{\cdot}05$. The right plot

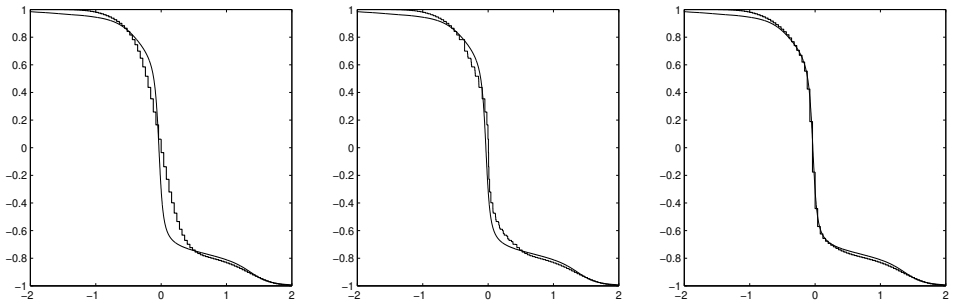

FIG. 1. Solution at time $t = 0{\cdot}3$ for $\varepsilon = 0{\cdot}1$ computed with 1 time step and $\Delta x = 0{\cdot}04$ by OS (left), COS(sc) with $\tau = 0{\cdot}15\Delta t$ (middle), and COS(md) (right). This corresponds to a CFL number 100. The reference solution is indicated by a thin line.

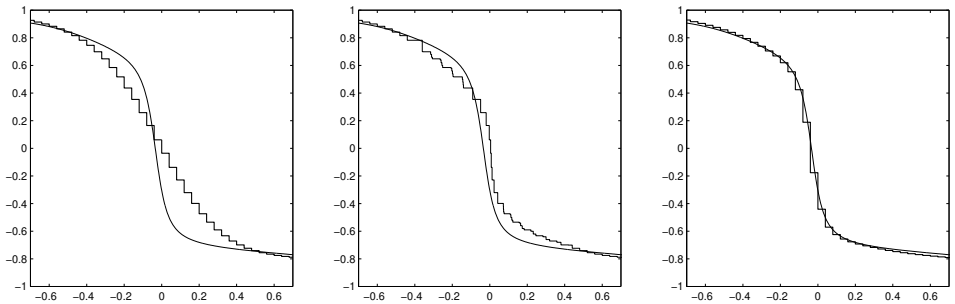

FIG. 2. The plots in Figure 1 magnified around the steep front.

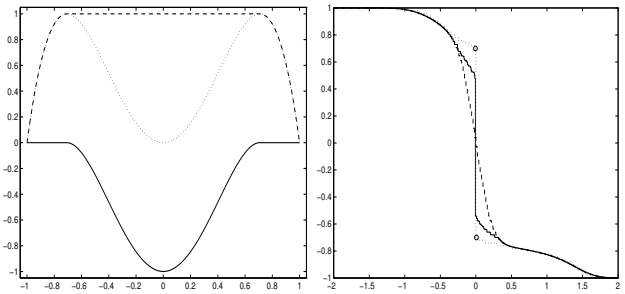

FIG. 3. (Left) The flux function (dotted), upper concave envelope (dashed), and residual flux function (solid) used by COS. (Right) Intermediate solutions for COS(sc) with separate correction for $\varepsilon = 0{\cdot}05$: advection solution (dotted), diffusion solution (dashed), and after correction (solid).

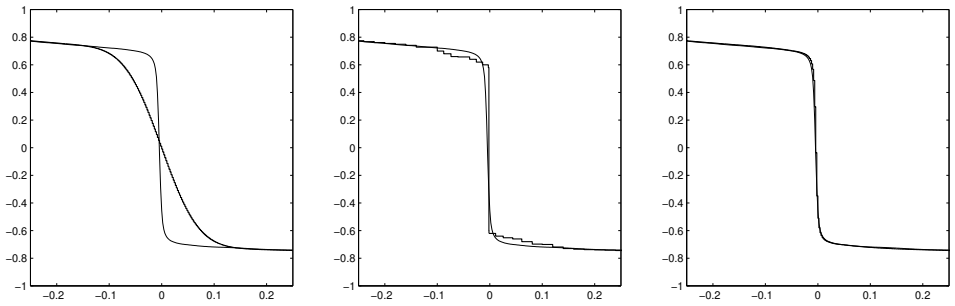

FIG. 4. Solution at time $t = 0{\cdot}3$ for $\varepsilon = 0{\cdot}005$ computed with 1 time step by OS (left), COS(sc) with $\tau = 0{\cdot}2\Delta t$ (middle), and COS(md) (right). The reference solution is indicated by a thin line. The grids are, from left to right, $\Delta x = 0{\cdot}002$, $0{\cdot}02$, and $0{\cdot}002$. (CFL numbers 2000, 200, 2000).

shows intermediate solutions for COS(sc). The strong shock where the correction operator is applied is indicated by circles (at y_i).

For comparison, Figure 4 shows a magnified part of the solution for $\varepsilon = 0{\cdot}005$ computed by the same three schemes as in Figure 1. Now, the time step is much larger than the diffusion scale and OS gives a considerable amount of splitting error, whereas the COS schemes resolve the front correctly. In the middle plot, the grid size ($\Delta x = 0{\cdot}02$) is chosen larger than the front width. Hence, the front is a subgrid phenomenon that is represented by a single discontinuity.

The conclusion of the above discussion is that the correction step implies that the accuracy at steep fronts is largely independent of the size of the time step, which contrasts strongly with standard splitting. The effect is even more pronounced for a larger time step ($\Delta t \gg \varepsilon$).

4.2 Example 2

In the next example we indicate the efficiency of the method. The operator splitting framework presented above uses a very simple explicit scheme for the diffusion and reaction steps. To get a fair comparison, we have therefore chosen to compare with an explicit finite difference scheme which uses Engquist–Osher differencing of the advection flux and central differencing of the diffusion flux, i.e.,

$$\begin{aligned} u_j^{m+1} &= -\beta V^{\Delta}(x_j,t_m)\big(f^-(u_{j+1}^m) - f^-(u_j^m) + f^+(u_j^m) - f^+(u_{j-1}^m)\big) \\ &\quad +\alpha u_{j-1}^m + (1-2\alpha)u_j^m + \alpha u_{j+1}^m, \end{aligned}$$

where $f^-(u) = \int \min\{f'(v),0\}dv$, $f^+(u) = \int \max\{f'(v),0\}dv$, $\beta = k/h$, and $\alpha = \varepsilon k/h^2$. The scheme is stable provided $\gamma = \beta \max|f'| + 2\alpha \leqslant 1$.

In practise, a more sophisticated method would be used for the diffusion step. Many such schemes are implicit and involve iterations to resolve the nonlinearities. For such schemes, isolating the advection in a separate step has certain advantages. First, a good initial guess is provided and second, some of the nonlinearity is removed. Hence, the iteration process converges in only a few iterations. This

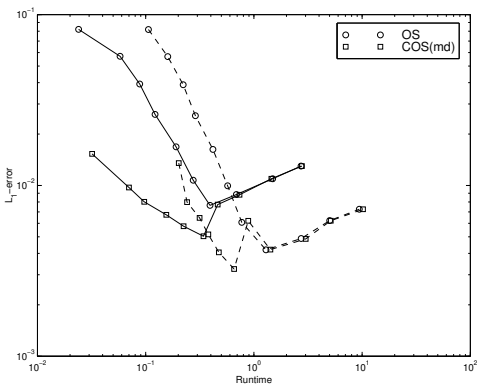

FIG. 5. Estimated L_1-error versus runtime for OS and COS(md) using 512 grid cells (solid line) and 1024 grid cells (dashed line).

has been documented in several studies for related operator splitting schemes; see Dahle (1988), Hansen & Espedal (1995), and Karlsen *et al.* If we were to compare such a realisation of our (corrected) operator splitting scheme with a conventional implicit method, the differences in efficiency would be even greater (in our favour) than what is demonstrated below.

The Engquist–Osher scheme has least numerical diffusion and optimal performance when γ is close to 1·0. Unfortunately, it is more difficult to ensure optimal performance (i.e., minimal error *and* runtime) for the operator splitting schemes, since the time steps can be chosen arbitrary. See Lie *et al* (1998) for a discussion of this topic. Here, we determine the optimal time step experimentally as follows. For a fixed spatial discretization, we measure L_1-error and runtime for 2^k time steps (for $k = 0, 1, \ldots$) and determine the optimum graphically.

Consider the same equation as in Example 1, now with $\varepsilon = 0{\cdot}01$. Figure 5 shows a plot of L_1-error versus runtime for OS and COS(md) with 512 and 1024 grid cells for both methods. We see that OS has a large error for few time steps. The error decreases with increasing number of time steps (increasing runtime) and reaches a minimum at 64 and 128 time steps, respectively. For larger number of time steps, the error increases due to increased numerical smearing introduced by the repeated projections after the advection steps. On the other hand, COS has a much lower error with one time step due to the improved resolution near the steep front. However, as mentioned in Example 1, one time step is not sufficient to resolve the solution to the left and to the right of the steep front, see Figure 1. Nevertheless, as the number of time steps increases, the overshoot disappears and an optimum (of error versus runtime) is observed for 32 time steps for both 512 and 1024 grid cells. With more steps, each time step is too short for a discontinuity to develop in the advection step. Hence, no correction is included and the performance drops to that of OS. Notice how the observations align neatly, indicating that the extra overhead introduced when determining possible corrections is negligible.

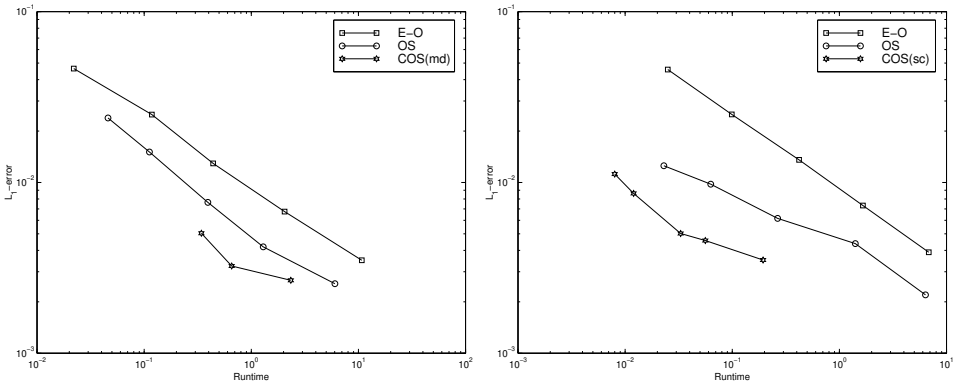

FIG. 6. Estimated L_1-error versus runtime for COS, OS, and the Engquist–Osher scheme for $\varepsilon = 0{\cdot}01$ (left) and $\varepsilon = 0{\cdot}001$ (right).

Figure 6 gives a comparison of the efficiency of the operator splitting schemes versus Engquist–Osher. The L^1-error is estimated from a reference solution computed by an explicit central difference scheme with 2^{15} grid cells. The number of grid cells were 2^n for $n = 7, \ldots, 11$. For OS and COS(md) the number of time steps were determined as in Figure 5. For COS(sc) we used one time step.

The conclusion of this example is that the operator splitting methodology provides an efficient (and accurate) numerical strategy.

4.3 Example 3

In the third example we determine experimental (asymptotic) order of convergence for the OS method. Note that OS and COS coincide when Δt becomes small, i.e., when the advection solutions do not contain shocks (see the above example). Consequently, we have chosen to focus our attention on the OS method in this example. To this end, consider (2) with $f(u) = u^2(1-u^2)$, $V(x) = 1 + 0{\cdot}5\sin(\pi x)$, and data $u_0(x) = \sin(\pi x)\chi_{[-1,1]}$. The domain is taken to be $[-2, 2]$ and solutions are computed up to time $t = 0{\cdot}5$. Table 1 shows measured L^1 errors and corresponding convergence rates for a numerical convergence study with fixed ratio between spatial and temporal discretization for $\varepsilon = 0{\cdot}1$, $0{\cdot}01$, and $0{\cdot}001$. The corresponding solutions are plotted in Figure 7. The errors are measured with respect to a piecewise constant solution (as used in the hyperbolic steps). The observed rates indicate a convergence rate of order one. But let us mention that second order rates are observed (results not shown here) if a Strang splitting is used together with a piecewise linear interpolation of the solution.

The splitting error is mostly a *temporal* error. In Table 2 we therefore show L^1 errors and convergence rates for an experiment with fixed spatial discretization. Also in this case the observed rates are of order one. A more thorough convergence study of the method (with constant coefficients and without source terms) is reported in Karlsen *et al.*

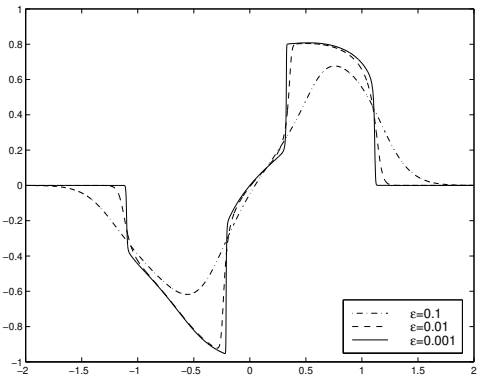

FIG. 7. Solution for three values of ε computed by OS on a fine grid.

TABLE 1
Numerical convergence rates for OS with fixed ratio between temporal and spatial discretization. N_x denotes the number of grid cells and N_t the number of time steps.

		$\varepsilon = 0{\cdot}1$		$\varepsilon = 0{\cdot}01$		$\varepsilon = 0{\cdot}001$	
N_x	N_t	L^1-error	rate	L^1-error	rate	L^1-error	rate
64	4	7·39e-02	—	1·34e-01	—	1·50e-01	—
128	8	3·70e-02	0·998	6·86e-02	0·966	7·55e-02	0·990
256	16	1·85e-02	1·000	3·46e-02	0·987	3·71e-02	1·025
512	32	9·32e-03	0·989	1·74e-02	0·992	1·88e-02	0·981
1024	64	4·71e-03	0·985	8·76e-03	0·990	1·00e-02	0·911
2048	128	2·40e-03	0·973	4·41e-03	0·990	5·33e-03	0·908

TABLE 2
Numerical convergence rates for OS with fixed temporal discretization $N_x = 2048$. N_t denotes the number of time steps

	$\varepsilon = 0{\cdot}1$		$\varepsilon = 0{\cdot}01$		$\varepsilon = 0{\cdot}001$	
N_t	L^1-error	rate	L^1-error	rate	L^1-error	rate
4	5·39e-02	—	1·03e-01	—	9·94e-02	—
8	2·76e-02	0·966	5·28e-02	0·964	5·24e-02	0·923
16	1·41e-02	0·969	2·68e-02	0·978	2·84e-02	0·884
32	7·28e-03	0·954	1·38e-02	0·958	1·55e-02	0·874
64	3·94e-03	0·886	7·38e-03	0·903	8·67e-03	0·838
128	2·40e-03	0·715	4·41e-03	0·743	5·33e-03	0·702

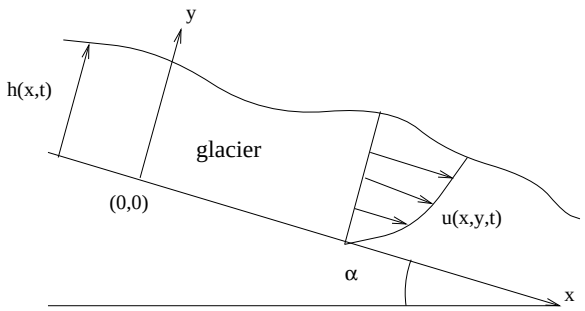

FIG. 8. A simplified model of a glacier

4.4 Example 4

In our fourth example we look at a simple one-dimensional model for glacier growth. Although the equations are realistic for describing a glacier, the computations are carried out for two simple examples. However, we wish to point out that our methodology is applicable for actual computations. In fact, it has been used in a study of Briksdalsbreen, which is a part of Jostedalsbreen (Norway) – the largest glacier in continental Europe.

A glacier with height $h(x,t)$ rests upon a flat mountain, making an angle α with the horizontal direction, see Figure 8. Following Fowler (1997), the flow is described by the conservation of mass and momentum in an incompressible flow. The stress tensor τ_{ij} is proportional to the strain rate; that is, $\tau_{ij} = \eta\dot{\epsilon}_{ij}$, where η is the effective viscosity. The strain rate is given by $\dot{\epsilon}_{ij} = 1/2(\partial u_i/\partial x_j + \partial u_j/\partial x_i)$. The glacier is a viscoplastic fluid, and the deformation is described approximately by an experimental relation called Glen's law; $\epsilon_{ij} = 1/2A\tau^{n-1}\tau_{ij}$, where the second stress invariant is given by $2\tau^2 = \sum_{ij}\tau_{ij}\tau ij$. The factor A generally depends upon the temperature, but here we assume that it is a constant. The exponent n is measured to be typically in the range 3–4.

We now adopt the shallow ice approximation; that is, we assume that the typical length scale l of the glacier is much larger than the typical depth d. Scaling variables and neglecting terms of lower order, Fowler derives the relation

$$\frac{\partial u}{\partial y} = A\big[1-\varepsilon h_x\big]^n (h-y)^n,$$

where $\varepsilon = d/l\cot\alpha$ is a small parameter. Letting u_b denote the sliding velocity at the bottom of the glacier, the volume flux becomes

$$u_b h + A\big[1-\varepsilon h_x\big]^n \frac{h^{n+2}}{n+2}.$$

The accumulation and ablation (melting) can be modelled by a source term $a(x,t,h)$. If we make the approximation that $(1-\varepsilon h_x)^n \approx 1 - n\varepsilon h_x$, we arrive

at the following equation

$$h_t + \left(u_b h + \frac{A}{n+2} h^{n+2}\right)_x - \left(\frac{n\varepsilon A}{n+2} h^{n+2} h_x\right)_x = a(x,t,h). \tag{32}$$

Here the diffusion term is nonlinear and of the form $\varepsilon(\nu(h)h_x)_x$, where the function $\nu(h)$ has a one-point degeneracy; that is, $\nu(0) = 0$. The degeneracy leads to finite speed of propagation of the interface between $h = 0$ and $h > 0$, i.e., the foot of the glacier. Operator splitting for advection-diffusion equations with a nonlinear, possibly strongly degenerate, diffusion term is analysed by Evje & Karlsen. Their analysis can be extended to cover the present case.

To define the operator splitting method, we write the glacier model on conservative form

$$h_t + f(h)_x = \varepsilon D(h)_{xx} + a(x,t,h),$$

where $D(h) = \int_0^h \nu(s)\,ds$. The equation is then split into a conservation law $h_t + f(h)_x = 0$ for the advection and a parabolic equation $h_t = \varepsilon D(h)_{xx} + a(x,t,h)$ for the diffusion and accumulation. The advective part is solved by front tracking and the parabolic equation is discretized by an explicit, central difference scheme.

We first look at a Riemann problem with $h(x,0) = \chi_{(-\infty,0]}$; a very simple model of an outlet into a valley. We are not interested in the glacier upstream and therefore use only a short interval of positive accumulation above zero ($x < 0$) and increasing ablation further downstream, We assume that the rate of accumulation and ablation (depending on the sign of the source term) only depends upon the altitude (i.e., on x), thus disregarding seasonal variations. To model this, we use the source $a(x,t,h) = a_0(x)$ if $h(x,t) > 0$ and $\max(a_0(x), 0)$ if $h(x,t) = 0$, where

$$a_0(x) = \begin{cases} (x + 0{\cdot}4)/2, & \text{for } x \in [-0{\cdot}4, -0{\cdot}2], \\ -x/2, & \text{for } x > -0{\cdot}2, \\ 0, & \text{otherwise.} \end{cases}$$

As a simple scaling we have used $u_b = 1/4$, $n = 4$, $A = (1 - u_b)(n + 2)$, and $\varepsilon = 0{\cdot}01$. Figure 9 shows three snapshots of the moving glacier front (snout). At times $t = 1{\cdot}0$ (left) and $t = 2{\cdot}0$ (middle) the snout is advancing, while at $t = 4{\cdot}0$ (right) it has reached a stationary state where the ablation balances the forward movement. In all plots the grid is uniform with 128 grid cells and we used 128 time steps to advance the solution up to time $t = 4{\cdot}0$ (corresponding to a CFL number approximately equal 10). The reference solution was computed on a 2048 grid with 8192 time steps.

At times $t = 1{\cdot}0$ and $t = 2{\cdot}0$ small splitting errors are visible at the top of the steep glacier front. Note, however, the accurate representation of the foot. When the stationary state is reached, the splitting error is hardly visible. To resolve the balance of advection and accumulation (and diffusion) properly, Δt is chosen to be of the same order as the diffusion scale ε. Hence, no entropy corrections are included in the simulation.

Second, we look at the growth of a new glacier. The glacier is to be restricted

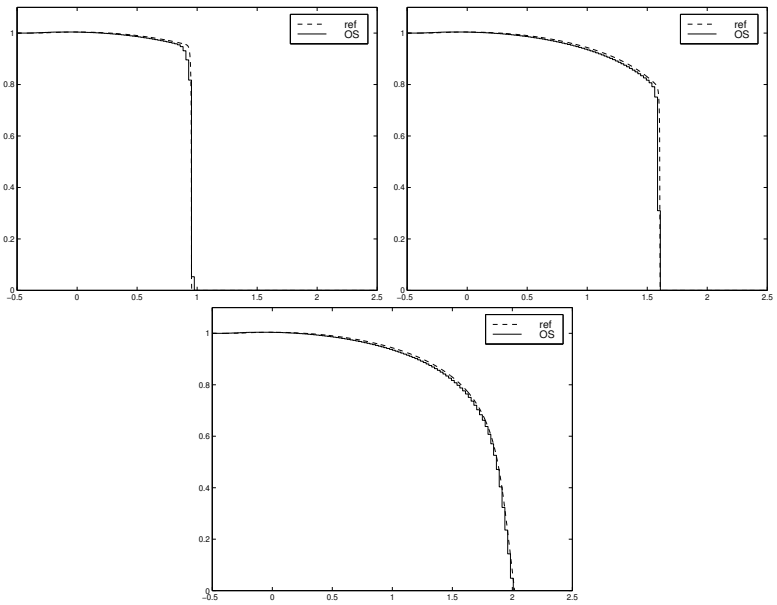

FIG. 9. Snapshots of a moving glacier at times $t = 1{\cdot}0$, $t = 2{\cdot}0$, and $t = 4{\cdot}0$ computed with OS on a 128 grid with 128 time steps.

approximately to the interval $[-5, 5]$, and hence we use the source term,

$$a(x,t) = \begin{cases} -0{\cdot}01x + 0{\cdot}05\sin(2\pi t), & x > -5{\cdot}0, \\ 0, & x < -5{\cdot}0. \end{cases}$$

Here the second term models seasonal variations; zero accumulation at the top in the middle of summer and no ablation at the bottom in the middle of winter. Figure 10 shows snapshots of a very accurate simulation of the glacier growth. The solution is computed by OS on a grid with 2 400 nodes using 20 000 time steps to reach time $t = 50{\cdot}0$. This corresponds to a CFL number $2{\cdot}3$. In the last plot the glacier has reached a steady profile (except for small seasonal variations).

Figure 11 shows the seasonal variations in the growing glacier. During the winter (from time $t = 10{\cdot}0$ to $t = 10{\cdot}5$) snow has accumulated on top of the glacier. Then the top melts down during the summer (from $t = 10{\cdot}5$ to $t = 11{\cdot}0$). Notice especially, the 'heap' of snow in front of the main glacier, which melts during the summer.

REFERENCES

ARBOGAST, T., & WHEELER, M. F. 1995 A characteristic-mixed finite element method for advection-dominated transport problems. *SIAM J. Num. Anal.* **32,** 404–424.

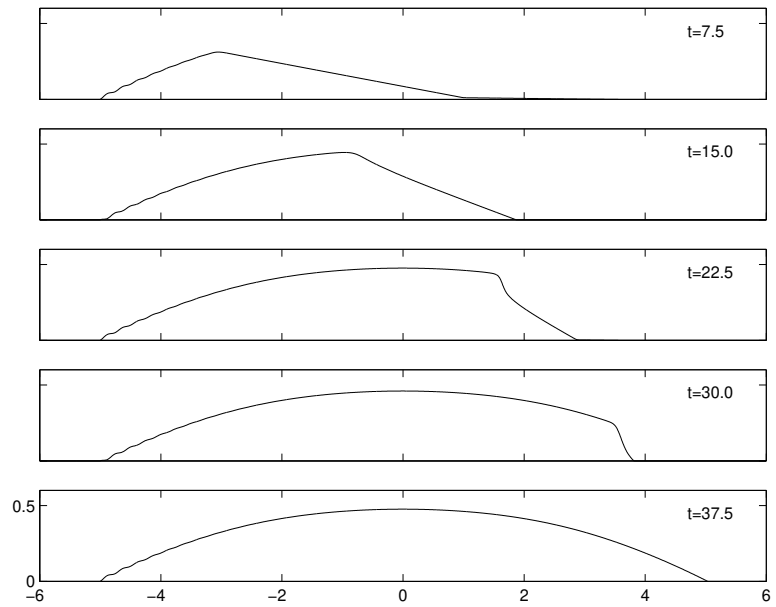

FIG. 10. Profile of a growing glacier.

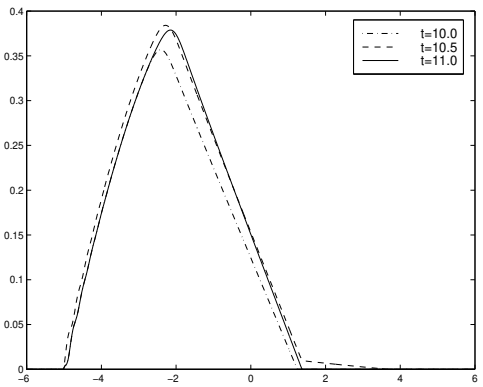

FIG. 11. Seasonal variations in the glacier profile

BEAR, J., & VERRUIJT, A. 1987 *Modeling groundwater flow and pollution.* Dordrecht: Reidel.

BLACK, F., & SCHOLES, M. 1973 The pricing of options and corporate liabilities. *Jour. Pol. Econ.* **81,** 637–659.

BURGERS, J. M. 1974 *The nonlinear diffusion equation.* Dordrecht: Reidel.

CELIA, M. A., RUSSELL, T. F., HERRERA, I., & EWING, R. E. 1990 An Eulerian-Lagrangian localized adjoint method for the advection-diffusion equation. *Adv. Water Resources* **13,** 187–205.

CHELLA, R., & OTTINO, J. M. 1983 Modelling of rapidly-mixed-fast-crosslinking exothermic polymerizations. *AIChE J.* **29,** 373–382.

COCKBURN, B., & SHU, C.-W. 1998 The local discontinuous Galerkin method for time-dependent convection–diffusion systems. *SIAM J. Num. Anal.* **35,** 2440–2463.

CRANDALL, M. G., & MAJDA, A. 1980 The method of fractional steps for conservation laws. *Numer. Math.* **34,** 285–314.

CRASTA, G., & PICCOLI, B. 1997 Viscosity solutions and uniqueness for systems of inhomogenous balance laws. *Discrete Contin. Dynam. Systems* **3(4),** 477–502.

DAFERMOS, C. M. 1972 Polygonal approximation of solutions of the initial value problem for a conservation law. *J. Math. Anal. Appl.* **38,** 33–41.

DAHLE, H. K. 1988 *Adaptive characteristic operator splitting techniques for convection-dominated diffusion problems in one and two space dimensions.* PhD thesis, Department of Mathematics, University of Bergen.

DAWSON, C. N. 1991 Godunov-mixed methods for advective flow problems in one space dimension. *SIAM J. Num. Anal.* **28(5),** 1282–1309.

DAWSON, C. N. 1995 High resolution upwind-mixed finite element methods for advection–diffusion equations with variable time-stepping. *Numer. Methods Partial Differential Equations* **11,** 525–538

DAWSON, C. N., VAN DUIJN, C. J., & WHEELER, M. F. 1994 Characteristic-Galerkin methods for contaminant transport with non-equilibrium adsorption kinetics. *SIAM J. Num. Anal.* **31,** 982–999.

DEMKOWITZ, L., & ODEN, J. T. 1986 An adaptive characteristic Petrov-Galerkin finite element method for convection-dominated linear and nonlinear parabolic problems in two space variables. *Computer Methods in Applied Mechanics and Engineering* **55,** 63–87.

DOUGLAS, J., & RUSSELL, T. F. 1982 Numerical methods for convection-dominated diffusion problems based on combining the method of characteristics with finite element or finite difference procedures. *SIAM J. Num. Anal.* **19(5),** 871–885.

ESPEDAL, M. S., & EWING, R. E. 1987 Characteristic Petrov-Galerkin subdomain methods for two-phase immiscible flow. *Comput. Methods Appl. Mech. Engrg.* **64** 113–135.

EVJE, S., & KARLSEN, K. H. Viscous splitting approximation of mixed hyperbolic-parabolic convection-diffusion equations. *Numer. Math.* to appear.

EWING, R. E. 1991 Operator splitting and Eulerian-Lagrangian localized adjoint methods for multiphase flow. In Whiteman, editor, *The Mathematics of Finite Elements and Applications VII MAFELAP*, 215–232. San Diego: Academic press.

EWING, R. E., & RUSSELL, T. F. 1982 Efficient time stepping methods for miscible displacement problems in porous media. *SIAM J. Num. Anal.* **19,** 1–67.

FOWLER, A. C. 1997 Glaciers and ice sheets. In J. I. Diaz, editor, *The Mathematics of Models for Climatology and Environment*, *NATO ASI Series* **48,** 302–336, Springer Verlag.

GODLEWSKI, E., & RAVIART, P.-A. 1996 *Numerical approximation of hyperbolic systems of conservation laws.* Springer Verlag.

HANSEN, R., & ESPEDAL, M. S. 1995 On the numerical solution of nonlinear reservoir flow models with gravity. *International Journal for Numerical Methods in Engineering* **38,** 2017–2032.

HERRERA, I., EWING, R. E., CELIA, M. A., & RUSSELL, T. F. 1993 Eulerian-lagrangian localized adjoint methods: The theoretical framework. *Numer. Methods Partial Differential Equations* **9,** 431–457.

HOFF, D., & SMOLLER, J. 1985 Error bounds for finite-difference approximations for a class of nonlinear parabolic systems. *Math. Comp.* **45(171),** 35–49.

HOLDEN, H., HOLDEN, L., & HØEGH–KROHN, R. 1988 A numerical method for first order nonlinear scalar conservation laws in one-dimension. *Comput. Math. Applic.* **15(6–8),** 595–602.

HOLDEN, H., & RISEBRO, N. H. 1998 *Front tracking for conservation laws.* Lecture notes, Norwegian University of Science and Technology, Trondheim.

HOLDEN, H., and RISEBRO, N. H. 1997 Conservation laws with a random source. *Appl. Math. Optim.* **36(2),** 229–241.

KARLSEN, K. H., BRUSDAL, K., DAHLE, H. K., EVJE, S., & LIE, K.-A. The corrected operator splitting approach applied to a nonlinear advection–diffusion problem. *Comput. Methods Appl. Mech. Engrg.* To appear.

KARLSEN, K. H., LIE, K.-A., RISEBRO, N. H., & FRØYEN, J. 1998 A front-tracking approach to a two-phase fluid-flow model with capillary forces. *In Situ* **22(1),** 59–89.

KARLSEN, K. H., & RISEBRO, N. H. Corrected operator splitting for nonlinear parabolic equations. *SIAM J. Num. Anal.* To appear.

KARLSEN, K. H., & RISEBRO, N. H. 1997 An operator splitting method for convection-diffusion equations. *Numer. Math.* **77(3),** 365–382.

LANGSETH, J. O., TVEITO, A., & WINTHER, R. 1996 On the convergence of operator splitting applied to conservation laws with source terms. *SIAM J. Numer. Anal.* **33(3),** 843–863.

LEVEQUE, R. J. 1992 *Numerical methods for convservation laws.* Basel: Birkhäuser Verlag, Lectures in Mathematics. ETH Zürich. 1992.

LIE, K.-A. 1997 *A front tracking method for one-dimensional nonlinear advection equations with variable coefficients.* Preprint. Mathematics No. **16**, Norwegian University of Science and Technology, Trondheim, Norway.

LIE, K.-A., HAUGSE, V., & KARLSEN, K. H. 1998 Dimensional splitting with front tracking and adaptive grid refinement. *Numer. Methods Partial Differential Equations* **14,** 627–648.

LIGHTHILL, M. J., & WHITHAM, G. B. 1955 On kinematic waves. II. Theory of traffic flow on long crowded roads. *Proc. Roy. Soc.* **229A,** 317–345.

MOCK, M. S. 1983 *Analysis of mathematical models of semi-conductor devices.*

Dublin: Boole Press.

MOHANTY, K. K., OTTINO, J. M., & DAVIS, H. T. 1982 Reaction and transport in disordered composite media. *Chem. Eng. Sci.* **37,** 905–924.

OLEINIK, O. A. 1963 Discontinuous solutions of non-linear differential equations. *Amer. Math. Soc Transl. Ser. 2*, **26,** 95–172.

RISEBRO, N. H. 1993 A front–tracking alternative to the random choice method. *Proc. Amer. Math. Soc.* **117(4),** 1125–1139.

RUSSELL, T. F. Galerkin time stepping along characteristics for Burgers' equation. In Stepleman et al., editor, *Scientific computing*, 183–192. IMACS, North-Holland.

RUSSELL, T. F. & TRUJILLO, R. V. 1990 Eulerian-Lagrangian localized adjoint methods with variable coefficients in multiple dimensions. In G. Gambolati et al., editor, *Proc. 8th Int. Conf. on Computational Methods in Water Resources*, 357–363. Southampton: Computational Mechanics Publications.

STRANG, G. 1968 On the construction and comparison of difference schemes. *SIAM J. Numer. Anal.* **5(3),** 506–517.

TRANGENSTEIN, J. A. 1995 Adaptive mesh refinement for wave propagation in nonlinear solids. *SIAM J. Sci. Comput.* **16(4),** 819–839.

WANG, H., DAHLE, H. K., ESPEDAL, M. S., EWING, R. E., SHARPLEY, R. C., & MAN, S. An ELLAM scheme for advection-dispersion equations in two dimensions. *SIAM J. Sci. Comput.* To appear.

WANG, H., & EWING, R. E. 1995 Optimal-order convergence rates for ELLAM for reactive transport and contamination in groundwater. *Numer. Methods Partial Differential Equations* **11,** 1–35.

WANG, H., EWING, R. E., & CELIA, M. A. 1995 Eulerian-Lagrangian localized adjoint methods for reactive transport with biodegradation. *Numer. Methods Partial Differential Equations* **11,** 229–254.

WANG, H., EWING, R. E., & RUSSELL, T. F. 1995 Eulerian-Lagrangian localized adjoint methods and their convergence analysis. *IMA J. Numer. Anal.* **15.**

WHEELER, M. F., KINTON, W. A., & DAWSON, C. N. 1988 Time-splitting for advection-dominated parabolic problems in one space variable. *Comm. Appl. Numer. Methods.* **4,** 413–423.